Micellization Activity of the Natural Lipopeptide [Glu_1, Asp_5] Surfactin-C15 in Aqueous Solution

Aihua Zou,[†,‡] Jing Liu,[†] Vasil M. Garamus,[‡] Ying Yang,[†] Regine Willumeit,[‡] and Bozhong Mu*[,†]

State Key Laboratory of Bioreactor Engineering and Institute of Applied Chemistry, East China University of Science and Technology, Shanghai 200237, P.R. China, and GKSS Research Center, Max-Planck-Str.1, 21502 Geesthacht, Germany

Received: September 8, 2009; Revised Manuscript Received: December 17, 2009

Surface tension, small angle neutron scattering (SANS), freeze-fracture transmission electron microscopy (FF-TEM), and circular dichroism (CD) have been used to study the self-aggregation properties of the natural lipopeptide [Glu_1, Asp_5] surfactin-C15 in 0.01 M phosphate buffer solution (PBS) at pH 7.4. It has been found that the critical micelle concentration (cmc) of surfactin is 1.54×10^{-5} M, the surface tension at the cmc (σ_{cmc}) is 27.7 mN/m, and the area per molecule at the air−water interface is 107.8 $Å^2$. Surfactin molecules adopt a β-sheet conformation already at low concentrations. This feature probably makes it surface-active at such low concentrations. From SANS and FF-TEM results, it is seen that surfactin exhibits a strong self-assembly ability to form sphere-like micelles and some larger aggregates even at the rare low concentration. The aggregation number of sphere-like micelles is much smaller than that for conventional surfactants of similar alkyl chain length.

Introduction

Surfactin, which is secreted by various strains of *Bacillus subtilis*, is one of the most powerful biosurfactants so far known. It is a cyclic lipoheptapeptide containing seven amino acids and a β-hydroxy fatty acid. Due to its amphiphilic structure, it can largely reduce the surface tension of water from 72 to 27 mN/m at a concentration of 1×10^{-5} M.[1,2] It is a strong foaming agent and a powerful emulsifier[3,4] and exhibits a strong membrane destabilizing action. Besides the surface activities, surfactin has also shown ionophoric and sequestering properties.[5,6] More importantly, surfactin exhibits significant biological activities, such as antiviral,[7,8] antibacterial,[9,10] anti-HIV,[11] antitumor,[12,13] and hemolytic[13,14] activities. Compared with the chemically synthesized surfactants, surfactin is gaining an enormous interest because they are less toxic, more biodegradable, and diverse. All of these properties make surfactin a very attractive compound for both industrial applications and biological studies.

The above physicochemical and biological properties are closely related to the mode of molecular assembly of surfactin in aqueous solution and the conformation of the surfactin molecules in the aggregates. Knoblich et al. discovered the micellar shape and size of surfactin changed with the pH values and the addition of ions by electron cryo-transmission electron microscopy (cryo-TEM).[15] Hsin-Hui et al. researched the aggregation of surfactin, at interfaces and in solution by neutron reflectivity measurement and SANS experiments.[16] They found that the structure of the micelle is of the core−shell type with the hydrocarbon chain and the four hydrophobic leucines forming the core of the micelle (pH 7.5). Han et al. observed that surfactin has a strong self-assembly ability to form micelles and the micelles tend to form larger aggregates.[17] Vass et al. found surfactin had the ability of adopting strongly different conformations depending on the conditions.[18] Bonmatin et al. found that in aqueous solution the peptide ring of surfactin shows a "horse-saddle" topology. The two negatively charged amino acid residues Glu and Asp constitute a minor polar domain. On the opposite side, Val residue extends down, facing the fatty acid chain, making up a major hydrophobic domain.[19]

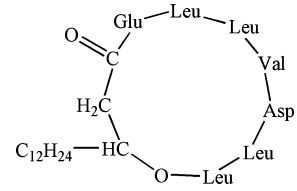

Figure 1. The chemical structure of surfactin.

Understanding the physical properties of naturally occurring surfactin not only helps in understanding their biological role but also is of considerable importance for applications in medicine (e.g., antibacterial or antitumor) and in the development of sustainable products (e.g., home and personal care products). However, it is not easy to identify clearly the hydrophobic and hydrophilic regions of the molecule, and also the experimental information about its aggregation properties, due to the complex structure of surfactin. These aspects inspire us to explore the micellization activity of [Glu_1, Asp_5] surfactin-C15 in PBS (pH 7.4) by surface tension, FF-TEM, SANS, and CD measurements. At the same time, we compare the previous study of surfactin's surface activities with our results in this paper.

Experimental Section

Materials. The [Glu_1, Asp_5] surfactin-C15 isoform (Figure 1) consists of a heptapeptide headgroup with the sequence Glu-Leu-Leu-Val-Asp-Leu-Leu closed to a lactone ring by a β-hydroxy fatty acid with 15 carbons. It was originally obtained

* Corresponding author. E-mail: bzmu@ecust.edu.cn.
† East China University of Science and Technology.
‡ GKSS Research Center.

10.1021/jp908675s
Published on Web 02/10/2010

from the cell free broth of *Bacillus subtilis* HSO121 in our laboratory.[20,21] The separation process for the surfactin is done according to refs 22 and 23. These lipopeptides were separated by extraction with methanol and isolation with a normal pressure ODS C18 column and purified by the RP-HPLC (Jasco Company, Japan). Then, the structure of the isolated lipopeptide was determined by the electrospray ionization-time-of-flight mass spectrometer (ESI-TOF MS/MS) and GC/MS.

Double distilled water was used for preparation of all solutions, except D_2O was used for the sample preparation of SANS measurements.

Surface Tension Measurements. The surfactin was dissolved in 0.01 M PBS (pH 7.4). Surface tension measurements were determined at 25.0 °C with a DCA 315 series system (Thermo-Cahn Instruments, Inc. USA). Prior to the measurements, the equipment was tested by determination of a surface tension of $\sigma = 72.7 \pm 0.2$ mN/m for double distilled water at 25.0 °C. The surface tension vs concentration plot was used to determine cmc and σ_{cmc}.

Origin 7.0 software was used to fit these curves and to determine the cmc, pre-cmc slope, and surface tension of the concentration at which micelles are formed according to the function

$$f(C_S) = -\frac{\partial\sigma}{\partial \ln C_S}(\ln \text{cmc} - \ln C_S)g(C_S) + \sigma_{cmc} \quad (1)$$

with $g(C_S) = 1$ for $C_S \leq$ cmc and $g(C_S) = 0$ for $C_S >$ cmc, where σ_{cmc} is the surface tension at the cmc and $\partial\sigma/\partial \ln C_S$ describes the alteration in the surface tension as a function of the natural logarithm of the surfactin concentration C_S (slope). The cmc, σ_{cmc}, and $\partial\sigma/\partial \ln C_S$ were used as fitting parameters in a least-squares fit. All values were reported as the mean and standard deviation according to the fitting curves. The excess surface concentration Γ can be calculated as[24]

$$\Gamma = -\frac{1}{kRT}\left(\frac{\partial\sigma}{\partial \ln(C_S)}\right) \quad (2)$$

where σ is the surface tension (N/m), R is the gas constant, T is the temperature in (K), and C_S is the surfactant concentration (mM). In the case of ionic surfactants, counterions were considered by setting k to 3.[24] From the maximum excess surface concentration, the headgroup area per molecule at the air−water interface (A) in ($Å^2$) was calculated by

$$A = (\Gamma \cdot L)^{-1} \quad (3)$$

where L is Avogadro's number. The free energy associated with the micelle formation per mole of monomer unit (ΔG^0_M) is evaluated according to the equation[25]

$$\Delta G^0_M = RT \ln \text{cmc} \quad (4)$$

Langmuir−Blodgett Technique. Surfactin was dissolved to a final concentration of 0.24 mM in a solution of chloroform/hexane (1/2, v/v). 100 μL of the stock solution was spread onto PBS buffer surfaces (pH 7.4) at 25 °C. The monolayer was maintained without compression for 30 min to complete the solvent evaporation and then was compressed at a rate of 0.1 $nm^2 \cdot min^{-1} \cdot molecule^{-1}$. Each of the isotherms was performed in triplicate, and the isotherms were reproducible.

Small Angle Neutron Scattering (SANS). 0.01 M phosphate buffer (pD 7.4) was used to prepare the samples. SANS measurements were performed on the instrument SANS-1 at Geesthacht Neutron Facility GeNF, Geesthacht, Germany.[26] To cover the range of scattering vectors q from 0.005 to 0.25 $Å^{-1}$, four sample-to-detector distances between 0.7 m < d < 9.7 m were used. Samples were kept in quartz cells (Hellma) with a path length of 2 mm and placed in a thermostatted sample holder to ensure isothermal conditions of $T = 25.0 \pm 0.5$ °C. Raw data were corrected for background from the deuterium buffer solution, sample cell, and other sources according to conventional procedures described in detail by Cotton.[27] The two-dimensional isotropic scattering spectra were azimuthally averaged, converted to an absolute scale, and corrected for the detector efficiency by dividing the incoherent scattering spectra of pure H_2O in quartz cell.[28] The scattering functions were interpreted using scaling concepts. The simple interpretation was enhanced by numerical modeling to certain geometric shapes.

The data were analyzed further by indirect Fourier transforms (IFT) by Glatter[29] in approximation of spherelike objects ($q > 0.02$ $Å^{-1}$) and trace scattering ($q < 0.02$ $Å^{-1}$) from large aggregates. IFT is a model independent approach and requires only a minimum of prior information for analysis, i.e., the maximum size and dimensions of aggregates (spherical, rod-like, or disk-like). The IFT method makes it possible to calculate the pair distance distribution function of scattering excess $p(r)$ for spherical aggregates. From the $p(r)$ function, the radius of gyration of the scattering length density excess R_g for spherical aggregates can be obtained.[30] From the shape of the curve obtained by plotting $p(r)$ against the distance, the shape of the micelle can be estimated. A symmetrical shape is related to spheres.

The aggregation number was calculated assuming that only surfactant molecules contribute to the micellar size and particularly to the micellar volume and scattering length density. The scattering length densities were calculated using table values from the studies by Chevalier and Zemb.[31]

Circular Dichroism (CD). The secondary structure of surfactin was probed by a Jasco J-810 circular dichroism spectropolarimeter at 25 ± 0.1 °C. The far-UV CD spectra of the surfactin at different concentrations were recorded in the range 190−260 nm with a spectral resolution of 0.1 nm. The scan speed was 100 nm/min, and the bandwidth was 2 nm. A quartz cell with an optical path of 0.1 cm was used. The final spectra were obtained by subtracting the surfactin spectra from the related PBS and then converting it to molar ellipticity ($deg \cdot cm^2 \cdot dmol^{-1}$) by its program.

Freeze-Fracture Transmission Electron Microscopy (FF-TEM). FF-TEM was used to characterize the morphology of surfactin aggregate in PBS (pH 7.4). The sample was placed in a specimen holder, maintained at the temperature (77 K) by liquid nitrogen. Then, the sample was rapidly transferred into the vacuum chamber of the freeze-etching apparatus (BALZERS BAF-400D) for fracturing. Fracturing was achieved by displacing a microtome arm cooled by liquid nitrogen to 100 K, when the pressure was less than 1×10^{-6} Pa. The now-exposed fracture face was immediately shadowed 2 nm platinum at an angle of 45° and 10−20 nm carbon at vertical direction. The specimens were washed in water, and then, the replicas were observed with a transmission electron microscope (JEM-1400, JEOL, Japan) at 20 000 magnification.

Results and Discussion

Adsorption of Surfactin onto Interface Geometric Properties. Surfactin carries two negative charges at pH 7.4 because the pK_a values of Asp and Glu are around 4.3 and 4.5,

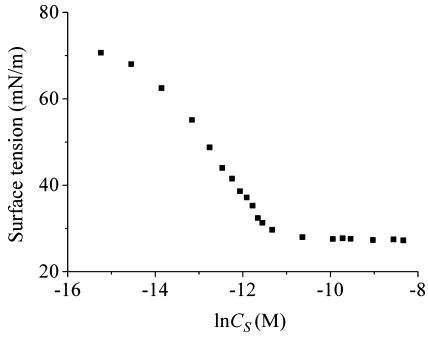

Figure 2. Surface tension isotherm of surfactin in 0.01 M PBS medium at 25 °C.

TABLE 1: Adsorption of Surfactin at the Air−Aqueous Solution Interface and Data Calculated from the Pre-cmc Slope

cmc (M)	1.54×10^{-5}
σ_{cmc} (mN/m)	27.7
$\partial\sigma/\partial \ln C_S$ (mM/m)	11.45
A^a (Å^2)	107.8
ΔG^0_M (kJ/mol)	−27.47
$V_C{}^b$ (Å^3)	350.2
$l_C{}^c$ (Å)	16.68
$CPP_S(V_C/l_CA)^d$	0.19
shape	sphere
$N_A{}^e$	11

[a] Head group area was calculated from the pre-cmc slope. [b] Carbon chain volume was calculated using $V_C = 27.4 + 26.9n_C = 350.2$. [c] Extended chain length was calculated with $l_C = 1.5 + 1.265n_C = 16.68$.[34] [d] Critical packing parameter (CPP_S) was calculated with $CPP_S = V_C/l_CA$. [e] Aggregation number N_A was calculated with $N_A = 36\pi(V_C)^2/(A)^3$.

respectively. Figure 2 is the surface tension isotherm for pure surfactin in pH 7.4 PBS, in which the cmc value of surfactin can be determined as 1.54×10^{-5} M. The cmc value of 1.54×10^{-5} M is relatively low in comparison with that of other ionic surfactants, which indicates that surfactin has a much stronger self-assembly ability. This result is similar to the results reported in references. Ishigami et al. found that surfactin forms large rod-shaped micelles having a cmc of 9.4×10^{-6} M in 0.1 M $NaHCO_3$ (pH 8.7).[1] Han et al. reported the surfactin has a cmc value of 3.8×10^{-5} M in pH 7.4 PBS by microcalorimetry.[17]

Information obtained by fitting of the individual surface tension curves, including the cmc, surface tension above the cmc, the pre-cmc slope, the area occupied by the molecule to micelle (A), and the free energy of micellization, are listed in Table 1. The calculation showed that the area per molecule at the air−water interface (A) is 107.8 Å^2 and the free energy of micellization is −27.47 kJ/mol, which indicates the compact surface structure of surfactin at the air−water interface.[16,32]

Maget-Dana and Ptak also used the surface tension to determine A for the [Asp_1, Glu_5] surfactin with a C14 chain.[32] Their application of the Gibbs equation to the surface tension gave a value of A of 132 Å^2 for the ionized molecule at concentrations close to the cmc, somewhat higher than our experimental value of 107.8 Å^2. The difference may be from the experimental conditions such as electrolytes in solution, pH, temperature, and the chain length of surfactin. However, both our and Maget-Dana's results are lower than Hsin-Hui Shen's experimental value of 147 Å^2 obtained from neutron reflection at the air−water interface.[16] According to the value of A (147 Å^2) determined by neutron reflection, Hsin-Hui Shen suggested that the chain must be folded back into the leucines of the heptapeptide ring and interacts strongly with the side chains of the hydrophobic amino acids, although the neutron results do not indicate with which residues the chain interacts.[16]

The shape of the aggregates formed by surfactant in solution is determined by the critical packing parameter (CPP_S):

$$CPP_S = \frac{V_C}{Al_C} \tag{5}$$

where V_C is the hydrophobic unit volume (normally carbon chain volume), A is the headgroup area, and l_C is the fully extended chain length of the molecule.[33] From the pre-cmc slope, the headgroup area per molecule was calculated (Table 1). For the calculations, the β-hydroxy fatty acid chain was taken as hydrophobe and peptide ring as hydrophile. Therefore, we assumed that the chain length totaled 12 carbon atoms for surfactin, and the carbon-chain volume and the extended chain length were calculated according to the method described by Tanford.[34] The details of the calculation are summarized in Table 1, and a CPP_S value of 0.19 was obtained. This result would mean that spherical micelles were the preferred type of surfactin aggregate, with an unbelievable low aggregation number of 11. The CPP_S value obtained here is similar to the result reported by Hsin-Hui Shen, in which they gave a CPP_S value of 0.21.[16] However, they gave one other estimate for the geometrical packing parameter of surfactin, which took the leucines and chain as the hydrophobic unit and gave a value of 0.65. This result would mean that a lamellar structure is favored for the surfactin aggregates.

The aggregation number of surfactin solution is unusually small at 11, which is quite different from the result obtained under more or less comparable conditions by Knoblich et al.[15] These authors found that surfactin forms large rod-shaped micelles (micellar weight, 179 000, aggregation number N_A = 173) having a cmc of 9.4×10^{-6} M and a surface tension at the cmc (σ_{cmc}) of 30 mN/m in 0.1 M $NaHCO_3$ (pH 8.7). However, our result is similar to the result of 20 obtained by neutron reflectivity at pH 7.5.[16] Compared with traditional ionic surfactant SDS (C12 and surface area 45 Å^2), the SDS micelles have an aggregation number of around 60 in aqueous solution.[35] Therefore, the small aggregation number for surfactin micelles sounds acceptable because it has a large surface area (107.8 Å). To examine this issue further, we will determine the structure of the surfactin aggregates later using SANS.

Furthermore, we have examined the behavior of surfactin molecules at the air−water interface. This was performed by carrying out the $\pi-A$ isotherm measurement by the Langmuir−Blodgett technique. Figure 3 shows $\pi-A$ curves of the insoluble monolayers of surfactin spread on buffer surfaces (pH 7.4) at 25 °C. The surface pressure in Figure 3 starts to increase apparently from an area of A_0 at 231 Å^2/molecule and reaches a breaking point at an area of A_t (123 Å^2/molecule). The surface pressure becomes constant on further compression of the monolayer. From the value of A_0 and A_t, it is obvious that the surfactin forms a very compact unit. The value of A obtained by the application of the Gibbs equation to the surface tension gave a value of 107.8 Å^2 for surfactin at concentrations close to the cmc. Therefore, it should be compared with A_t from the $\pi-A$ curve. It is obvious that both values are almost consistent with each other.

The pattern of our curve (Figure 3) is similar to that of the isotherms observed by Song et al[20] and Marget-Dana et al.[32]

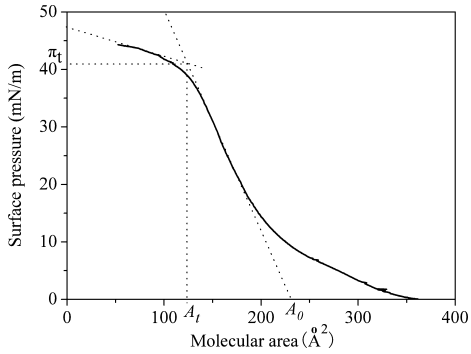

Figure 3. $\pi-A$ isotherm of surfactin monolayer at subphase pH 7.4 (25 °C).

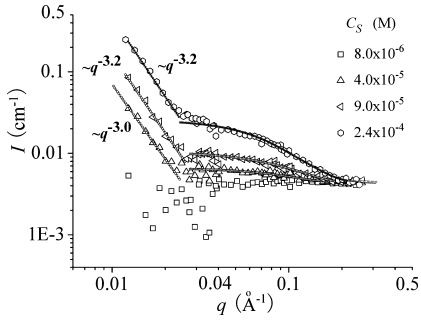

Figure 4. SANS spectra of surfactin solution at different surfactin concentrations.

Our A_0 and A_t values are more or less similar to the values obtained from their reported curves. The difference is because of the subphase pH and the chain length of surfactin. Maget-Dana and Ptak,[32] Ishigami et al.,[1] and Gallet et al.[36] measured values of A_0 and A_t at low pH, where the surfactin is not ionized. Their values range from 154 to 215 Å^2 for A_0 and from 89 to 132 Å^2 for A_t (for the surfactin with a C14 chain). Maget-Dana et al. have explained their results by suggesting that the surfactin molecules are compressed from A_0 to A_t with a molecular orientation in which both the peptide rings and the alkyl chains lie flat on the water surface.[32] Gallet et al. concluded that surfactin adsorbed with the plane of the peptide ring aligned with the surface and that the most stable structure at the interface was one with the chain folded back so as to interact with leucine 2 and valine 4.[36]

Small Angle Neutron Scattering. SANS data were collected for surfactin solutions in D_2O at a temperature of 25 °C. The obtained scattering curves are dependent on surfactin concentration (shown in Figure 4). The scattering intensity increases with the surfactin concentration. For the lowest concentration at 8.0 $\times$ 10^{-6} M, there is almost no regular scattering at a q range (0.01−0.024 Å^{-1}). This result is consistent with the surface tension measurement, because this concentration (8.0 $\times$ 10^{-6} M) is lower than the cmc value.

We started the analysis of the scattering data for other surfactin concentrations, by applying the indirect Fourier transformation (IFT) method developed by Glatter,[29] using the version reported by Pedersen.[37] This model-independent approach needs only minor additional (model) information on the possible aggregate structure: dimensions (spherelike, rodlike, or disklike) and a maximal value of the diameter, cross-sectional diameter, or thickness, respectively.

First observation of scattering curves suggests that there are three regions, i.e., (i) at the lowest q range ($q < 0.02$ Å^{-1}), there is strong decay of scattering intensity as power law $q^{-\alpha}$ ($\alpha > 2$) and we consider this scattering as trace scattering of large object; (ii) at intermediate q region (0.02−0.07 Å^{-1}), the scattering intensity decreases quite slowly similar to the Guinier approximation $\exp(-R_g^2q^2/3)$ with $R_gq < 1$; (iii) at large q region ($q > 0.1$ Å^{-1}), there we see $q^{-\alpha}$ again. Scattering at intermediate and large q range we attribute to smaller objects with a typical size of the order of $1/q \sim 50$ Å.

TABLE 2: Results of SANS Data Analysis by a Model-Independent Approach (IFT), Model Fitting, and Calculated Parameter of Aggregates for Surfactin Solution ($T = 50$°C)

surfactin (M)	D_{max} (Å)	R_g (Å)	$I_{(0)}$ (cm^{-1})	N_A[a]
4.0×10^{-5}	50	16 ± 0.4	0.0021 ± 0.0006	11
9.0×10^{-5}	50	16.9 ± 0.7	0.0058 ± 0.0003	12
2.4×10^{-4}	60	20.1 ± 0.6	0.021 ± 0.0006	18

[a] N_A: Aggregation number calculated by $N_A = I_{(0)}L/(C_{surfactin} - cmc)M_{surfactin}\Delta\rho_m^2$.

The IFT routine for spherelike aggregates was applied to the large q part ($q > 0.02$ Å^{-1}). At the large q range ($q > 0.02$ Å^{-1}), the experimental data and the fitted curves coincide very well (Figure 4). The obtained Gaussian shape of the pair distribution function is characteristic of almost-homogeneous sphere-like aggregates formed by surfactin. Here, we got the estimation of the micelle diameter D_{max}, which is obtained from the maximum distance of $p(r)$. After determination of the pair distance distribution function, the radius of gyration of the scattering length density excess R_g and the aggregation number N_A for sphere-like micelle were calculated (Table 2).

Table 2 shows the micelle diameter (D_{max}) and the gyration radius (R_g) changes with the surfactin concentration. The surfactin aggregation number is unbelievably small (less than 20). However, this result is similar to the results reported by Hsin-Hui Shen et al.[16] They find that the aggregation number at pH 7.5 is at 20 $\pm$ 4 with an overall micelle diameter of 50 $\pm$ 5 Å and a gyration radius of 22 $\pm$ 2 Å by means of SANS. They argue that the structure of the spherical micelle is of the core−shell type with the hydrocarbon chain and the four hydrophobic leucines forming the core of the micelle.

At a q range of 0.01−0.02 Å^{-1}(except 8.0 $\times$ 10^{-6} M surfactin), evidence for fractals in the submicrometer and nanometer scale can be conveniently derived from SANS (Figure 4) based on well-known dimensional analysis.[37] The power law of the scattering intensity $I(q)$ can be described as

$$I_{(q)} \sim q^{-\alpha} \tag{6}$$

where the exponent indicates whether the microscopic structure of the scatterer can be understood as mass fractals or surface fractals. When the angular coefficient of the log $I(q)$ vs log q plot is determined, it correlates to the dimensions of mass and surface fractals, D_V and D_S, as

$$\alpha = 2D_V - D_S \tag{7}$$

If $1 < \alpha < 3$, the scattering curve can be associated with mass fractal material. In these systems, which are often referred to as volume or bulky fractals, the surface and volume have the same fractal dimension, i.e., $D_V = D_S$. The volume (V) and the surface area (S) of the particle are related to the dimensions D_V and D_S as

$$V(r) \sim r^{D_V} \tag{8}$$

and

$$S(r) \sim r^{D_S} \tag{9}$$

If $3 < \alpha < 4$, the scattering curve can be associated with surface fractal material. Such particles have a dense core and rough surface. The core has a Euclidean dimension, $D_V = 3$, whereas the surface obeys the relation $D_S = 6 - \alpha$.

If $\alpha = 4$, the material is not fractal but has a uniform, dense core with a perfectly smooth surface. This relates to the dimensions as $D_V = 3$ and $D_S = 2$.

Figure 4 plots SANS data of surfactin solution as well as the fits to the IFT models with assumption of the trace contributions of large fractal objects ($q < 0.02$ Å^{-1}). It can be seen that the curves for 4.0×10^{-5}, 9.0×10^{-5}, and 2.4×10^{-4} M decay as $\sim q^{-3.0}$, $\sim q^{-3.2}$, and $\sim q^{-3.2}$ at low q (<0.02 Å^{-1}), respectively. Thus, the above decays fall within the limits of 3 and 4. This is an indication of fractal-like surface regions,[38] characterized by fractal dimension for expected surface around 2.8. The above results point to the fractal interface between aggregates formed by surfactin and the surrounding solvent. Therefore, surfactin forms not only simple micelles but large aggregates as well even at very low concentration. Most probably, these are some sheets of surfactin bilayers, which will form a lamellar phase with a further increase of surfactin concentration. Here, we stress that the fractal type scattering characteristics are not unique but could in principle arise also from a specific type of size distribution of the objects. Our SANS results should be compared with the results reported by Hsin-Hui Shen et al.,[16] where only the spherical micelles with an overall micelle diameter of 50 ± 5 Å and a gyration radius of 22 ± 2 Å have been found by SANS for the fully protonated surfactin and the deuterated leucine version both in D_2O at 1 mM. We also observed micelles of such size at slightly low concentration (0.24 mM) but together with much larger aggregates.

SANS data may indicate that in the considered q range ($q < 0.02$ Å^{-1}) the material is dominated by a certain fractal type. However, as scattering gives an average picture of the material, the coexistence of different kinds of fractals cannot be excluded. Furthermore, polydispersity of aggregates can affect the obtained values of fractal dimension. Due to the above certain limitations of SANS experiments, FF-TEM was performed to observe the morphology of surfactin solution. The morphology of surfactin aggregates at 4.0×10^{-5} and 2.4×10^{-4} M was shown in Figure 5, where different shapes of micelles are observed, and proves the existence of large aggregates. It is abnormal that at low surfactin concentration the bilayered unilamellar structure was found in Figure 5A (arrow) and also the wormlike micelles coexisted. This is a similar result from that obtained under more or less comparable conditions using cryo-TEM by Knoblich et al.[15] These authors found that surfactin micelles are not homogeneous but inhomogeneous with regard to size distribution with different configurations. The different types of micelles from spherical to ellipsoidal and/or cylindrical with diameters in the range 4−20 nm and lengths of up to 160 nm were revealed at pH 7, 9.5, and 12 by cryo-TEM. The large ellipsoidal and/or cylindrical are thought to consist of bilayered unilamellar or bilayered multilamellar structures. In addition, Ishigami and co-workers also reported that a micellar surfactin solution in 0.1 M $NaHCO_3$ (pH 8.7) forms micelles of large size from the measurement of static light scattering.[1] They obtained an average length of 231 nm and diameter of 6 nm when the micelles were assumed to be cylindrical. Han et al. observed the bimodal distribution of the hydrodynamic radius by the dynamic light scattering measurements in terms of the relative scattered intensity, with one peak at 4−6 nm and another broad peak centered at ∼108 nm for 0.3 mM surfactin.[17]

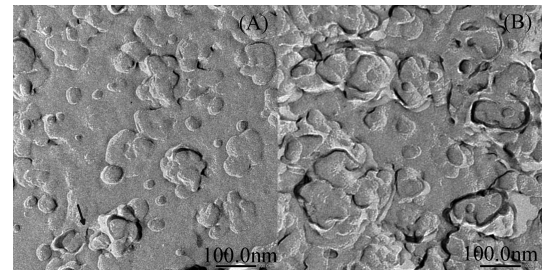

Figure 5. FF-TEM images of 4.0×10^{-5} M (A) and 2.4×10^{-4} M (B) surfactin in PBS (pH 7.4).

Surfactin formed large aggregates (fractal-like surface regions) even at a concentration of 9×10^{-5} M (6 times above the cmc). This can again be an indication that the strong hydrogen bond between the peptide loops of surfactin molecules, which makes the aggregation of surfactin micelle favorable, even at low concentrations. The CPP_S values calculated from the surface tension data suggested that surfactin forms spherelike micelles ($CPP_S \sim 0.19$), whereas there also exists some large aggregates found from SANS and FF-TEM results.

Hsin-Hui Shen et al. gave one other estimate for the geometrical packing parameter of surfactin, which took the leucines and chain as the hydrophobic unit and gave a value of 0.65.[16] This result would mean that a lamellar structure is favored for the surfactin aggregates, while their SANS analysis can be fit only with a self-consistent model when the leucines are in the hydrophobic core of the micelle. Therefore, they argue that surfactin is a molecule whose behavior is not easily described in terms of a packing parameter. The concept of a packing parameter is evidently difficult to apply with confidence to a molecule of this shape, so it may be more helpful to think of the surface properties of surfactin in terms of the factors that stabilize Pickering emulsions.[39]

CD Spectra of Surfactin Micelles. Surfactin is a kind of lipopeptide, with a peptide loop of seven amino acid residues and a β-hydroxy hydrophobic fatty acid chain. With some work reported previously, surfactin formed micelles with β-sheet structure. The typical β-sheet spectrum has a minimum at around 216 nm and a maximum at about 195 nm in the CD spectra.[40] These β-sheet type structures involve Leu_2-Leu_3-Val_4-Asp_5, and the structure is stabilized by a hydrogen bond between the carbonyl group of Leu_2 and the amide groups of Asp_5.[41] Nevertheless, this secondary structure of surfactin as a peptide may be affected by experimental conditions such as electrolytes in solution,[42] pH, temperature, the stability of the lactone ring under the experimental conditions, and interactions with other molecules.[43] Ishigami et al. found that the surfactin formed large rod micelles with β-sheet structure at low concentrations just around the cmc.[1] Osman et al. studied the effects of extrinsic environmental conditions on the conformation of surfactin to indicate that both surfactin monomers and surfactin micelles had a β-sheet conformation at a neutral pH value.[44] However, Maget-Dana et al. showed that the surfactin micelles had a turn conformation in pH 8.3 Tris buffer.[45] Yuchun Han et al. found that surfactin can display different secondary structures at different concentrations.[17] It mainly adopts the β-turn conforma-

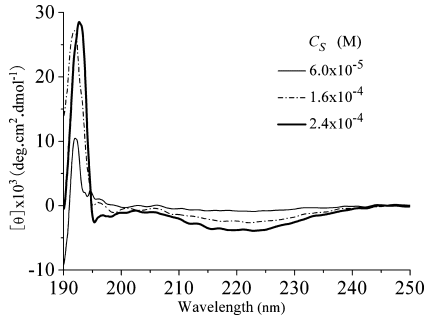

Figure 6. Far-UV CD spectra of surfactin at different concentrations in PBS (pH 7.4).

tion at relative low micelle concentration, whereas it adopts the β-sheet conformation at higher micelle concentration.

In the present work, circular dichroism measurements were performed to monitor the secondary structure of surfactin in pH 7.4 PBS (Figure 6). The spectra were scanned in the wavelength region 190−250 nm to probe transition in backbone amide. The CD spectrum of surfactin in Figure 6 has a negative peak at ∼220 nm and a maximum peak at ∼193 nm. With the surfactin concentration increasing, the corresponding molar ellipticity degree increases. Thus, surfactin forms β-sheets as a secondary structure in our systems and the β-sheet formation is enhanced by increasing the surfactin concentration. The β-sheet of surfactin may depend on an intermolecular hydrogen bond. Thus, the large aggregates in surfactin solution may arise from the intermolecular interactions of surfactin within the triple balance of ionic, hydrophobic−hydrophilic, and hydrogen bonding properties.

Conclusions

The combination of different analytical standard methods (surface tension, SANS, FF-TEM, and CD measurements) gave a comprehensive characterization of the physical properties of surfactin in 0.01 M PBS (pH 7.4).The natural lipopeptide [Glu$_1$, Asp$_5$] surfactin-C15 has a cmc of 1.54×10^{-5} M and an area per molecule of 107.8 Å^2. The $\pi-A$ isotherm of surfactin at the air−water interface was obtained by the Langmuir−Blodgett technique, which shows that the surface pressure starts to increase apparently from the area of A_0 at 231 Å^2/molecule and reaches a breaking point at the area A_t of 123 Å^2/molecule. These results mean that this natural biosurfactant surfactin has a strong self-assembly ability and forms a compact surface structure at the air−water interface.

The structure of surfactin micelles has been identified by means of SANS and FF-TEM. The SANS data can be divided into two main sections. For $q \geq 0.02$ Å^{-1}, the scattering curves are interpreted to stem from sphere-like domains; for $q < 0.02$ Å^{-1}, SANS data shows the existence of large fractal objects. Therefore, surfactin forms not only simple micelles but also large aggregates as well even at very low concentration. The aggregation number of 20 was found to be unusually small for the sphere-like micelles. The coexistence of sphere-like micelles, wormlike micelles, and bilayered unilamellar structure was found in this natural lipopeptide solution at relatively low concentrations. This result points out that the packing parameter is difficult to apply with surfactin. CD measurements show that surfactin adopts a β-sheet conformation at micelle concentrations.

Surfactin's special surface activity may be used as a basis for its biological role such as the antiviral, antibacterial, and antitumor activities. A variety of models and potential mechanisms have been proposed for its biological activity, such as strong membrane permeabilization, the formation of a channel, and the detergent-like action. Thus, its biological role is related to its strong self-assembly ability even at low concentration. Our study could lead to new ideas for the potential application of surfactin in health care and biotechnology.

Acknowledgment. The support of this work by the Alexander von Humboldt Foundation, by Research Fund for the New Teacher of the Doctoral Program of Higher Education of China (200802511024), and by the grant from the Ministry of Science and Technology of China (2007CB707801) is gratefully acknowledged.

References and Notes

(1) Ishigami, Y.; Osman, M.; Nakahara, H.; Sano, Y.; Ishiguro, R.; Matsumoto, M. *Colloids Surf., B* **1995**, *4*, 341–348.
(2) Peypoux, F.; Bonmatin, J. M.; Wallach, J. *Appl. Microbiol. Biotechnol.* **1999**, *51*, 553–563.
(3) Deleu, M.; Razafindralambo, H.; Popineau, Y.; Jacques, P.; Thonart, P.; Paquot, M. *Colloids Surf., A* **1999**, *152*, 3–10.
(4) Razafindralambo, H.; Paquot, M.; Baniel, A.; Popineau, Y.; Hbid, C.; Jacques, P.; Thonart, P. *J. Am. Oil Chem. Soc.* **1996**, *73*, 149–151.
(5) Thimon, L.; Peypoux, F.; Michel, G. *Biotechnol. Lett.* **1992**, *14*, 713–718.
(6) Thimon, L.; Peypoux, F.; Wallach, J.; Michel, G. *Colloids Surf., B* **1993**, *1*, 57–62.
(7) Itokawa, H.; Miyashita, T.; Morita, H.; Takeya, K.; Hirano, T.; Homma, M.; Oka, K. *Chem. Pharm. Bull.* **1994**, *42*, 604–607.
(8) Vollenbroich, D.; Özel, M.; Vater, J.; Kamp, R. M.; Pauli, G. *Biologicals* **1997**, *25*, 289–297.
(9) Beven, L.; Wroblewski, H. *Res. Microbiol.* **1997**, *148*, 163–175.
(10) Vollenbroich, D.; Pauli, G.; özel, M.; Vater, J. *Appl. Environ. Microbiol.* **1997**, *63*, 44–49.
(11) Weislow, O. S.; Kiser, R.; Fine, D. L.; Bader, J.; Shoemaker, R. H.; Boyd, M. R. *J. Natl. Cancer Inst.* **1989**, *81*, 577–586.
(12) Kameda, Y.; Matsui, K.; Kato, H.; Yamada, T.; Sagai, H. *Chem. Pharm. Bull.* **1972**, *20*, 1551–1557.
(13) Kameda, Y.; Ouhira, S.; Matsui, K.; Kanatomo, S.; Hase, T.; Atsusaka, T. *Chem. Pharm. Bull.* **1974**, *20*, 938–944.
(14) Bernheimer, A.; Avigad, L. *J. Gen. Microbiol.* **1970**, *61*, 361–369.
(15) Knoblich, A.; Matsumoto, M.; Ishiguro, R.; Murata, K.; Fujiyoshi, Y.; Ishigami, Y.; Osman, M. *Colloids Surf., B* **1995**, *5*, 43–48.
(16) Shen, H. H.; Thomas, R. K.; Chen, C. Y.; Darton, R. C.; Baker, S. C.; Penfold, J. *Langmuir* **2009**, *25*, 4211–4218.
(17) Han, Y. C.; Huang, X.; Cao, M. W.; Wang, Y. L. *J. Phys. Chem. B* **2008**, *112*, 15195–15201.
(18) Vass, E.; Besson, F.; Majer, Z.; Volpon, L.; Hollósi, M. *Biochem. Biophys. Res. Commun.* **2001**, *282*, 361–367.
(19) Bonmatin, J. M.; Genest, M.; Labbe, H.; Ptak, M. *Biopolymers* **1994**, *34*, 975–986.
(20) Song, C. S.; Ye, R. Q.; Mu, B. Z. *Colloids Surf., A* **2007**, *302*, 82–87.
(21) Namir, H.; Liu, X. Y.; Yang, S. Z.; Mu, B. Z. *Protein Pept. Lett.* **2008**, *15*, 265–269.
(22) Liu, X. Y.; Namir, H.; Yang, S. Z.; Mu, B. Z. *Protein Pept. Lett.* **2007**, *14*, 766–773.
(23) Liu, X. Y.; Yang, S. Z.; Mu, B. Z. *J. Pept. Sci.* **2008**, *14*, 864–875.
(24) Janczuk, B.; Zdziennicka, A.; Wojcik, W. *Colloids Surf., A* **2003**, *220*, 61–68.
(25) Zana, R. *Adv. Colloid Interface Sci.* **1995**, *57*, 1–64.
(26) Stuhrmann, H. B.; Burkhardt, N.; Dietrich, G.; Junemann, R.; Meerwinck, W.; Schmitt, M.; Wadzack, J.; Willumeit, R.; Zhao, J.; Nierhaus, K. H. *Nucl. Instrum. Methods* **1995**, *A356*, 133–137.
(27) Cotton, J. P. In *Neutron, X-ray, and Light Scattering-Introduction to an Investigative Tool for Colloidal and Polymeric Systems. Initial Data Treatment*; Lindner, P., Zemb, T., Eds.; North-Holland: Amsterdam, The Netherlands, 1991.
(28) Wignall, G.; Bates, F. *J. Appl. Crystallogr.* **1987**, *20*, 28–40.
(29) Glatter, O. *J. Appl. Crystallogr.* **1997**, *10*, 415–421.
(30) Feigin, L. A.; Svergun, D. *Structure Analysis by Small-Angle, X-Ray, and Neutron Scattering*; Plenum Press: New York, 1987.
(31) Chevalier, Y.; Zemb, T. *Rep. Prog. Phys.* **1990**, *53*, 279–371.
(32) Maget-Dana, R.; Ptak, M. *J. Colloid Interface Sci.* **1992**, *153*, 285–291.
(33) Israelachvili, J. N. *Intermolecular and Surface Forces*, 2nd ed.; Academic Press: London, 1992.

(34) Tanford, C. *The Hydrophobic Effect: Formation of Micelle and Biological Membranes*; Wiley and Sons: New York, 1980.
(35) Garamus, V. M. *Langmuir* **2003**, *19*, 7214–7218.
(36) Gallet, X.; Deleu, M.; Razafindralambo, H.; Jacques, P.; Thonart, P.; Paquot, M.; Brasseur, R. *Langmuir* **1999**, *15*, 2409–2413.
(37) Pedersen, J. S. *Adv. Colloid Interface Sci.* **1997**, *70*, 171–210.
(38) (a) Schmidt, P. W. *J. Appl. Crystallogr.* **1991**, *24*, 414–435. (b) Schmidt, P. W. Some Fundamental Concepts and Techniques Useful in Small-Angle Scattering Studies of Disordered Solids. In *Modern Aspects of Small-Angle Scattering*; Brumberger, H., Ed.; Kluwer Academic Publishers: Dordrecht, The Netherlands, 1995.
(39) Aveyard, R.; Binks, B. P.; Clint, J. H. *Adv. Colloid Interface Sci.* **2003**, *100*, 503–546.
(40) Yang, J. T.; Wu, C. S. C.; Martinez, H. M. *Methods Enzymol.* **1986**, *130*, 208–269.
(41) Bonmatin, J. M.; Genest, M.; Petit, M. C.; Gincel, E.; Simorre, J. P.; Cornet, B.; Gallet, X.; Caille, A.; Labbe, H.; Vovelle, F.; Ptak, M. *Biochimie* **1992**, *74*, 825–836.
(42) Matsumoto, M.; Uyeda, N. *Bull. Inst. Chem. Res., Kyoto Univ.* **1988**, *66*, 1635–1637.
(43) Wu, C. S. C.; Yang, J. T. *Mol. Cell. Biochem.* **1981**, *40*, 109–122.
(44) Osman, M.; Høiland, H.; Holmsen, H.; Ishigami, Y. *J. Pept. Sci.* **1998**, *4*, 449–458.
(45) Maget-Dana, R.; Ptak, M. *Biophys. J.* **1995**, *68*, 1937–1943.

JP908675S